Resonant Raman scattering in a bis-tetramethyltetraselenafulvalene-hexafluorophosphate [$(TMTSF)_2PF_6$] single crystal

M. Krauzman, H. Poulet, and R. M. Pick
Département de Recherches Physiques Université Pierre et Marie Curie 4, Place Jussieu 75005 Paris
(Received 22 July 1985)

Raman scattering experiments have been performed on a $(TMTSF)_2PF_6$ single crystal. Resonant effects have been found for a laser excitation in the vicinity of 6450 Å. The latter experiment has allowed us to detect and identify many internal modes of the TMTSF molecule. Also, external modes have been recorded and identified. One of them is strongly Raman resonant, and is responsible for the electronic charge transfer which characterizes this one-dimensional conductor.

I. INTRODUCTION

$(TMTSF)_2PF_6$ is a one-dimensional (1D) organic conductor, which remains metallic down to very low temperatures. At $T=10$ K, it becomes a magnetic insulator at normal pressure, while at 12 kbar, it undergoes a metal-superconductor transition at 0.9 K.[1] $(TMTSF)_2PF_6$ crystallizes in the space group $P\bar{1}$ [(2)] with $Z=1$; the PF_6 cation lies on an inversion center, while the TMTSF molecules form stacks along the a direction, the two molecules located in the same unit cell (corresponding to each other through an inversion center located at the center of the unit cell) belonging to the same stack.

The origin of metallic 1D conductivity in the series of $(TMTSF)_2X$ salts is well known. The TMTSF molecule acts as an electron donor, while the X counteranion is an electron acceptor. With a 2 to 1 stoichiometric ratio between the TMTSF and X, half an electron leaves each TMTSF molecule; the electronic band related to the donor state is thus half empty, leading to conducting properties. The nature of the very-low-temperature electronic and magnetic properties depends, nevertheless, on that of the X anion, which always resides on an inversion center. For $X=PF_6$ or AsF_6, the superconducting state is reached only under pressure,[1-3] but for $X=ClO_4$, this transition takes place at 0 kbar for $T=4$ K;[4] it has been suspected that the ordering of the ClO_4 ion at low temperature (which lowers the crystal symmetry) could be related to the different electric behavior of this latter compound.

There exists already considerable literature on the optical properties of the tetramethyltetrathiafulvalene (TMTTF) and of the TMTSF molecules, either neutral[3] or fully ionized.[4] In contrast, very few results exist for $(TMTSF)_2PF_6$ itself or even for closely related one-dimensional conductors such as $(TMTTF)_2PF_6$, for instance.

The present study was undertaken in order to fill this gap by studying the Raman spectrum of this substance. The initial goal was to record the internal modes of the PF_6 counterion in order to see whether some orientational disorder existed in this salt also and whether it could be, later on, correlated with the corresponding information on the ClO_4 internal modes. Unfortunately, the two salts turned out to be very opaque and no internal line of any counterion could be detected in them. On the other hand, some other lines, though weak, could be recorded and were discovered, at least some of them, to display resonant effects under a change of the excitation-laser wavelength. The aim of this paper is to report and discuss these findings. This paper will be divided as follows.

Section II describes the experimental technique and the normalization procedure used to display the four recorded spectra.

In Sec. III we summarize the various crystallographic and optical data which are available for $(TMTSF)_2PF_6$ and for some related substances and which are necessary for the interpretation of our experiment.

Section IV is devoted to a discussion of our experimental results; after a brief description of the various spectral regions and a review of resonant Raman scattering (RRS) theory, we apply the latter to these different spectral regions and show that many of our results can be properly interpreted within such a framework.

Finally, Sec. V is devoted to a summary of the important results so far obtained (in particular, the demonstration of resonant Raman scattering with one external mode of the crystal), as well as to a discussion of the still unsolved questions raised by the present work.

II. EXPERIMENTAL PROCEDURES AND TECHNIQUES

Our Raman experiments were performed with a T 800 Coderg spectrometer. We equipped it with a large-aperture light-collecting system designed in such a way that it provides a magnification of 3.5 from the sample to the spectrometer entrance slit, with a frontal distance of 21 cm from the scattering system to the first lens. The spectrometer was electrically connected through a laboratory-made interface to a Digital Equipment Corporation PDP 11/03 computer, controlling the scans and allowing for data collection and treatment. Two Spectra Physics 164 lasers (argon and krypton) were used to produce the excitation light.

The crystals we used resembled prismatic black needles. These needles had four planar faces, each parallel to the a direction, with a surface area of approximately 8×0.2 mm^2. The small size of these faces, as well as the very

low intensity of the scattered light, forced us to use special devices in order to ensure that all the light arriving on the entrance slit was Raman-scattered light originating from our sample. In order to prevent the detection of Raman scattering from other sources, two crystals were installed horizontally, side by side, and carefully fixed with 50-μm golden wires inside a groove in the holder of the cryostat, in such a way that one of their faces was vertical. The samples were cooled by the convection of a fixed volume of helium gas kept at constant pressure and in thermal equilibrium with the copper walls of the inner cell. The latter was brought to the appropriate temperature by an external helium flow. The three windows crossed by the incident laser beam and the three windows crossed by the scattered light were pure SiO_2 and carefully cleaned in order to avoid spurious fluorescence.

The samples can be very easily damaged by laser heating and another source of difficulty, especially in the case of RRS, was the additional presence, in the detected signal, of laser plasma lines elastically scattered by the crystal. The former difficulty was reduced and the latter totally overcome by the following system.

The laser was located far away (8 m) from the sample. The light passed through two lenses, constituting a beam-expander telescope, which sent the beam on a 10×10-cm^2, 1200-(vertical grooves)/mm blazed grating. The first-order diffracted beam was then sent back to the same grating via a mirror and was once more first-order dispersed. The beam, which covered about 50% of the surface of the grating was made to slowly converge in such a way that the focus of the system was located approximately 1 m in front of the sample. In fact, due to the optical aberrations of the system, this focus consisted of two caustics mutually orthogonal and both perpendicular to the beam. We made use of these aberrations by placing a vertical slit at the position of the vertical caustics, thus eliminating the plasma lines. The horizontal caustic was then imaged as a horizontal 5×0.1-mm^2 line on one face of the crystal, this line being itself imaged, by the above-described collecting optics, on the horizontal entrance slit of the spectrometer.

The characteristics of this system are a filtering spectral width of 4 cm^{-1} at half height, with an attenuation of 100 6 cm^{-1} away from the selected laser line, and the possibility of sending a light power of 40 mW on to the sample without noticeable heating. Even with such a power the spectra were very weak and, for instance, with a 4-cm^{-1} spectrometer spectral slit width, the 450-cm^{-1} line of the 4545-Å VV spectrum (Fig. 2) produced a signal of 5 counts/sec over a background of 100 counts/sec.

We used a horizontal, right-angle scattering geometry with a 60° incident angle with respect to the normal to a vertical face (containing the horizontal a direction) and a 30° mean scattering angle; a mask was placed between the sample and the entrance slit in order to prevent detection of the directly reflected light. The incident light was polarized vertically, i.e., perpendicular to a; the scattered light was analyzed either vertically (VV scattering) or horizontally (VH scattering) by a polaroid. A half-wave plate was placed behind the analyzer and turned, for each experiment and each wavelength in such a way that the outgoing light was polarized in the direction for which the spectrometer had its maximum efficiency. It was thus possible to compare, for each wave length, the VV and VH relative intensities. The relative intensities of the VH 4545- and 6471-Å spectra could not be experimentally decided. It was fixed by assuming an equal intensity for the 36-cm^{-1} line in both spectra, and the reason of this choice will be discussed in Sec. IV C.

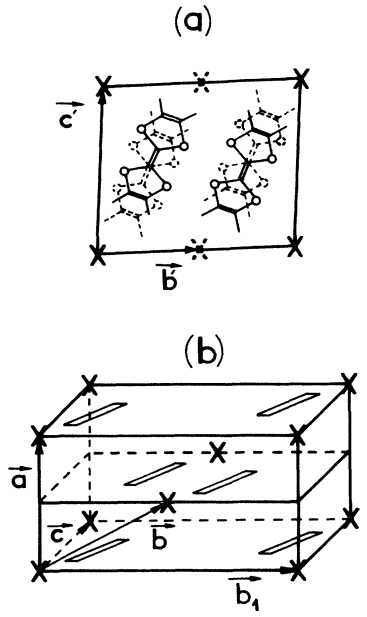

FIG. 1. (a) Projection along a of the pseudomonoclinic cell. The molecules in the plane $x=0$ are drawn as solid lines, while those in the plane $x=a/2$ are represented by dashed lines. The crosses are symbols for PF_6^- ions. b' and c' are the projections of b and c. (b) Sketch of the pseudomonoclinic cell where the TMTSF molecules are symbolized by parallelograms.

III. SUMMARY OF RELEVANT DATA ON $(TMTSF)_2PF_6$

A. Crystallography

As already explained, $(TMTSF)_2PF_6$ crystallizes in the space group $P\bar{1}$, with $Z=1$, and the two molecules correspond to each other through an inversion center located at the center of the cell. (When not otherwise stated, the word molecule will be used as an abbreviated form for "TMTSF molecule.") In fact, although the crystal has a very low symmetry, the structure analysis reveals that the molecules, which are stacked along a, are fairly planar; this plane being, within 1°, perpendicular to a and passing nearly through a phosphor atom (which lies on an inversion center). Furthermore, the distance between two molecules of the same cell and the distance between two molecules belonging to the same stack but to two neighboring unit cells is nearly the same (as pointed out in Ref. 2). Finally, the C axis is nearly perpendicular to a ($\beta=86.3°$). Thus, if one defines a new cell with basis vectors $a, b_1=-a+2b, c$ the crystal structure in this new cell is approximately C_{2h}^3 ($C(2/m),1,1$), each molecule being in

a mirror plane perpendicular to **a** and passing either through the origin, or through the center of the *c* face as shown in Fig. 1. The H geometry in the light scattering experiment is thus parallel to the twofold axis, while the V one is in the mirror plane. Finally, the data of Thorup *et al.*[2] also indicate that the local environment distorts the molecular shape very little: it nearly has the D_{2h} symmetry of the isolated molecule, and it is the latter which will be assumed for the vibrational properties of the molecule.

Let us finally note that this approximate C_{2h} crystal symmetry does not hold for the counterion (no P—F bond is close to alignment with *a*). This is of no importance here because this counterion does not manifest itself in our experiments.

B. Optical data

Several vibrational spectroscopy experiments have been performed, either on the neutral or on the fully ionized molecule (TMTSF ClO_4 and TMTSF Br). Iwahana *et al.*[5] reported some Raman measurements on TMTSF and $(TMTSF)_2PF_6$. Later on, Meneghetti *et al.*[6] performed ir and Raman experiments on the neutral molecule, as well as on TMTSF Br (ir) and TMTSF PF_6 dissolved in acetonitrile (Raman). From these data and from the corresponding data for TMTTF, Meneghetti *et al.* constructed a valence force field, which allowed them to compute all the in-plane internal-mode motions, assuming a D_{2h} molecular symmetry. This calculation led to agreement between the computed and some of the recorded frequencies (all the Raman detected frequencies being identified as modes of a_{1g} symmetry), some other recorded frequencies receiving no proper explanation. [Note that throughout this paper, lower-case symbols will be used for the irreducible representations of the molecular group D_{2h}, while capital letters will refer to the irreducible representations of the factor group of the crystal space group ($P\bar{1}$ or C_{2h}).] Meneghetti *et al.*[6] also pointed out that the Raman spectrum of the fully ionized molecule showed signs of RRS at $\lambda = 6471$ Å due to an electronic absorption, measured around 8000 Å in the acetonitrile solution and around 6500 Å in solid TMTSF ClO_4. They also reported another electronic absorption around 3800 Å in the solid.

Very few optical data are related, on the other hand, to the vibrational spectroscopy or the optical data of the half-ionized salts. Iwahana *et al.*[5] were only able to detect one Raman line of $(TMTSF)_2PF_6$ at 1463 cm^{-1}. The same line was measured on various salts of TMTTF by Huong *et al.*,[7] who reported that its frequency suffered a linear shift with the degree of ionization of the molecule.

An ir absorption experiment was also performed on $(TMTSF)_2X$ with $X = PF_6$ and ReO_4 by Bozio *et al.*[8] This ir experiment, which provided some frequencies for the Meneghetti *et al.*[6] calculation, is important in our case for the following reason. As the two TMTSF molecules of the unit cell are related by an inversion center, each internal vibration gives rise, in principle, to two modes: a Raman-active one and an ir-active one. Nevertheless, if the molecule keeps its local D_{2h} symmetry, a gerade vibration and, in particular, an a_{1g}-symmetry internal mode will be ir active only if the electron-vibration coupling is quite large.[9] In the experiment of Bozio *et al.*,[8] it was found that no a_{1g} internal mode could be detected in the metallic state, both for ReO_4 and PF_6. Few such modes were, indeed, detected in the insulating low-temperature phase for ReO_4, but none became visible under the same conditions with PF_6. This reinforces the idea of a regular stacking of the molecules, with practically no dimerization between the two molecules of the unit cell, as was implied in our pseudomonoclinic ($C(2/m),1,1$) cell.

An optical-absorption measurement was also performed by Jacobsen *et al.*[10] in the visible range on single crystals of $(TMTSF)_2X$, with $X = AsF_6$. The 6400-Å absorption band discussed above for the fully ionized salt was seen, on the PF_6 half-ionized one, as a small peak in reflectance measurements for light polarized perpendicular to the chain (V geometry). Due to the relationship with the Meneghetti *et al.*[6] electronic and Raman measurements, this absorption is presumably related to a transition from an occupied state to the valence band. On the other hand, no peak was observed in the H geometry, at that frequency, but the reflectance began to rise with no detected maximum in the 5000—4000-Å region.

C. Electronic structure analysis and related information

Two band-structure calculations have been performed on these materials by Whangbo *et al.*[11] and by Grant.[12] Both calculations were based on the linear-combination-of-molecular-orbitals (LCMO) method, which in fact included only the contribution of one single molecular orbital. This implies that for all the other electronic bands below the conduction band, and presumably also for the first electronic band above the conduction band, the same approximation is valid. In fact, the most important information pertinent to our measurements is related to the calculation of Grant who computed the transfer integrals of the molecular orbital related to the conducting state between one molecule and its various neighbors. He also computed the relative change of these transfer integrals with respect to a change of the relative position of the molecule within the cell. He found that the most dramatic change occurred in the transfer integral between two nearest-neighbor molecules belonging to the same stack but to two different cells when they were moving parallel to the *a* direction. This relative change was computed to be larger, by a factor of 4, than any other relative change of these transfer integrals.

IV. EXPERIMENTAL RESULTS AND DISCUSSION

Figure 2 represents an overview of four recorded spectra at 30 K for $\lambda = 4545$ Å and $\lambda = 6471$ Å, both for the VV and VH geometry. Figure 3 represents the low-frequency part of these spectra with an expanded frequency scale; Fig. 4 shows a detailed view of the 1400—1650-cm^{-1} part of the same spectra, with a reduced intensity scale, in order to show the relative intensity of the very active 1463-cm^{-1} line, with again an expanded frequency

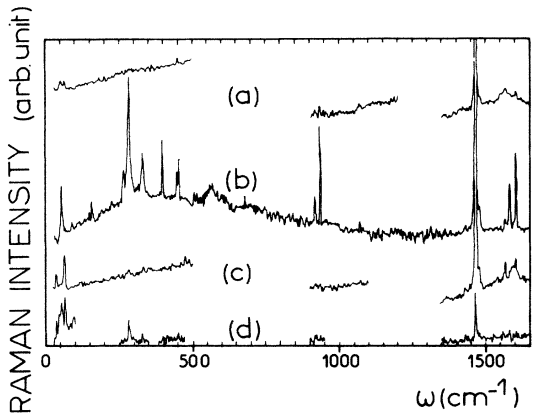

FIG. 2. Overview of four recorded spectra at 30 K of $(TMTSF)_2PF_6$. From top to bottom, the geometry and laser wavelength are the following: (a) VV and 4545 Å, (b) VV and 6471 Å, (c) VH and 4545 Å, and (d) VH and 4545 Å.

scale. These three figures make clear the two following points.

(i) The low-frequency part ($\omega < 100$ cm^{-1}) and the 1400—1600-cm^{-1} region behave in a different manner from the rest of the spectrum.

(ii) With the exception of the two above-mentioned spectral regions, the spectra are extremely weak, if not completely featureless, as was the case in the Iwahana experiment[5] for all geometries but the VV $\lambda = 6471$ Å one. The latter clearly appears as a RRS which provides a lot of results. Thus, we shall first give a short summary of the elements of RRS theory necessary for the interpretation of our results; second, apply it to the 150—1400-cm^{-1} region; third, discuss the external mode ($\omega < 100$ cm^{-1}) spectrum; and finally, describe the new problems which arise above 1400 cm^{-1}.

A. Resonant Raman scattering

Following Loudon,[13] the one-phonon Raman scattering phenomenon is made up of three processes: (1) photon annihilation plus creation of an electron-hole pair, (2) interaction of a phonon with one member of the pair, creating a different electron-hole pair, and (3) destruction of an electron-hole pair producing the scattered photon. These processes take place in any order, giving rise to six different orderings. One of these terms, corresponding to the three processes taking place in the order described above, is

$$R^{\alpha\beta j}(\omega_i) \simeq \sum_{\mathbf{k}} \frac{\langle v,\mathbf{k}|p_\alpha|c_1,\mathbf{k}\rangle\langle c_1,\mathbf{k}|Q|c_2,\mathbf{k}\rangle\langle c_2,\mathbf{k}|p_\beta|v,\mathbf{k}\rangle}{(\omega_{c_1}-\omega_v+\omega_{\rm ph}-\omega_i)[(\omega_{c_2}-\omega_v)-\omega_i]} , \quad (1)$$

where $|v,\mathbf{k}\rangle$ or $|c_i,\mathbf{k}\rangle$ are crystal electronic states with wave vector $\mathbf{k}$, related to a valence band (v) or a conduction band (c_i) labeled by the index i, $\hbar\omega_v$ and $\hbar\omega_{c_i}$ are the corresponding electronic eigenvalues, while $\omega_{\rm ph}$ is the scattered phonon frequency. In the numerator, p_α (p_β) is the dipole moment operator for a dipole parallel to the α (β) direction, while Q is the electron-phonon operator, which when applied to an electronic wave function, describes the way this wave function is perturbed under the influence of a phonon. (Note that we have neglected the light, and

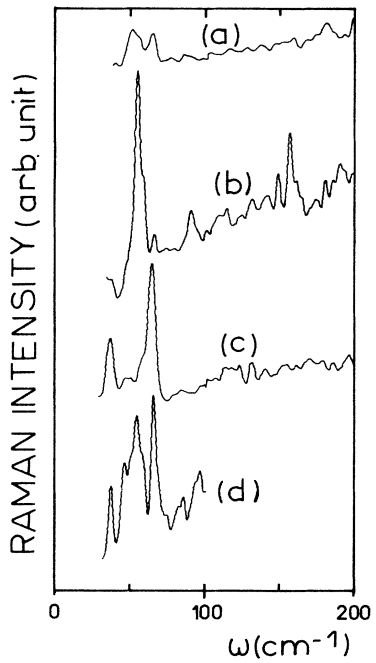

FIG. 3. External-mode region (0—200 cm^{-1}) of the spectra—presentation as in Fig. 2.

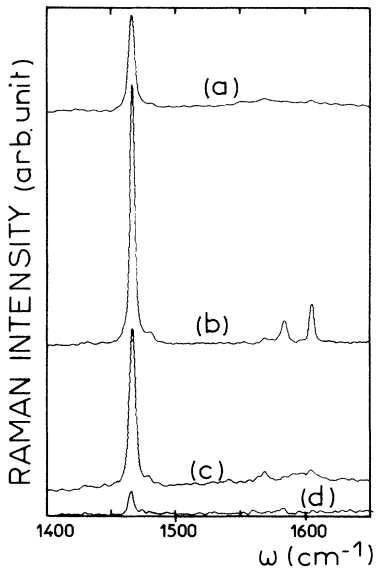

FIG. 4. 1400—1650-cm^{-1} part of the spectra, on a reduced intensity scale, showing the strong activity of the 1463-cm^{-1} line—presentation as in Fig. 2.

scattered-phonon, wave vector for simplicity.)

Resonant Raman scattering takes place when (neglecting the phonon energy) the photon energy is equal to the energy of an electron-hole pair. Equation (1) shows that in the Raman process described by this equation this can happen twice, once if $\omega_{c_1}-\omega_v=\omega_i$ and once if $\omega_{c_2}-\omega_v=\omega_i$.

The analysis of the Loudon formula shows that one has a similar result if the hole-phonon interaction takes place as the second scattering process, while this can happen once only if this interaction (or the electron-phonon interaction) is the first or the last process. The most strongly resonant term is thus (1) (or its equivalent where the roles of the conduction and valence band are interchanged) when the two conduction (valence) bands are the same,[14] in which case the Raman tensor diverges as $(\omega_c-\omega_v-\omega_i)^{-2}$.

In the LCMO method with one molecular orbital per band, one writes

$$|v,\mathbf{k}\rangle=\sum_{L,s}\phi_v(\mathbf{r}-\mathbf{R}_L^S)e^{i\mathbf{k}\cdot\mathbf{R}_L}\ , \tag{2}$$

where $\phi_v(\mathbf{r}-\mathbf{r}_0)$ is the v molecular orbital centered at $\mathbf{r}_0$, and $\mathbf{R}_L^s$ is the center of the s molecule ($s=1,2$) of the L cell. Then, at the same level of approximation,

$$\langle v,\mathbf{k}\,|\,p_\alpha\,|\,c,\mathbf{k}\rangle=\int 2N\phi_v^*(\mathbf{r})\frac{\partial}{\partial r_\alpha}\phi_c(\mathbf{r})d^3r\ . \tag{3}$$

As $\phi v(\mathbf{r})$ and $\phi c(\mathbf{r})$ can be classified by their D_{2h} symmetry properties, there exists for each (v,c) set, at most, one operator p_α for which the matrix element is different from zero.

Thus, in the LCMO method with one molecular orbital per band, the most strongly resonant terms impose $\alpha=\beta$, i.e., the incident- and scattered-light polarizations both have to be parallel to one and have the same given direction. Furthermore, the internal vibration modes are fairly localized on one molecule. The electron-phonon matrix element thus couples one molecular orbital with another one localized on the *same* molecule. As in the case of RRS, the orbitals both belong to the same band (see above), symmetry implies that the internal mode must belong to the totally symmetric (or identity) representation, a_{1g}. The corresponding rules for external modes will be discussed in Sec. IV C.

B. The 150–1400-cm^{-1} region: Identification of the internal modes

The optical-absorption measurements of Jacobsen *et al.*[10] suggest that RRS will appear for a laser frequency around 6471 Å in the VV geometry, and we have shown that we expect this resonant effect to be mostly important for a_{1g} modes. This is, indeed, largely the case and Table I lists, in column 1, the frequency of the modes detected in this geometry which can be attributed, with the help of the Meneghetti *et al.*[6] calculation (column 2), to a_{1g} modes. One sees that all the modes, with frequencies between 155 and 1620 cm^{-1} and attributed to a_{1g} symmetry in Ref. 6, are detected in our measurements, except for the ν_6 mode. Furthermore, the ν_7 and ν_{12} modes which were not previously detected turn out to have frequencies in rather good agreement with their predicted values (155 cm^{-1} for ν_{12} instead of a predicted 133-cm^{-1} value and 1070 for ν_7 instead of 1057 cm^{-1}). Also the 1464-cm^{-1}

TABLE I. Frequencies (cm^{-1}) of the modes detected above 130 cm^{-1}. Indications of their relative intensities are abbreviated as follows: w=weak, m=medium, and s=strong. Mode 1: resonant-mode frequencies which can be compared with the a_{1g} in-plane–mode calculated frequencies of Ref. 6 (mode 2 with the Meneghetti *et al.* labeling). Mode 3: nonresonant (VH) or poorly resonant modes. Mode 4: unidentified, strongly resonant, modes; the asterisk indicates modes already detected by other experimentalists. Mode 5: modes with special properties discussed in Sec. IV D.

Mode 1	Mode 2	Mode 3	Mode 4	Mode 5
155 (w)	133 (ν_{12})			
263 (w)	263 (ν_{11})			
281 (m)	276 (ν_{10})			
			328 (m)*	
			398 (m)	
452 (m)	453 (ν_9)			
		473 (w) (VH)		
		489 (w) (VH)		
		679 (w) [$\nu_{62}(b_{3g})$]		
918 (mw)	916 (ν_8)			
			936 (m)	
1070 (w)	1057 (ν_7)			
	1370 (ν_6)			
1452 (w)	1438 (ν_5)			
1464 (s)	1469 (ν_4)			
				1479 (mw)
				1565 (m)
			1582 (m)*	
1601 (m)	1625 (ν_3)			

value of ν_3 compares favorably with a predicted value (using the empirical law of Huong *et al.*) of 1469 cm^{-1}. Column 3 of the same table gives the frequencies of the two internal modes detected in nonresonant conditions in the VH spectrum and of one mode detected in the VV spectrum which seems to be poorly resonant. The latter can be identified with a b_{3g} (ν_{62}) mode of Ref. 6, while the two others are out-of-plane modes not computed by these authors. The surprising result is the appearance of the frequencies listed in column 4 (the case of column 5 will be discussed in Sec. IV D), which correspond to frequencies appearing under RRS (VV geometry) and which cannot be accounted for by the Meneghetti *et al.* calculation. Two of them, marked with an asterisk, have already been reported in earlier measurements[5,6] and are not identified. The fact that they are strongly resonant is quite surprising. They could be combination bands (with two phonons of the same or of different frequencies) of the same symmetry, but there exists no indication of their origin, in particular, for the 324- and 398-cm^{-1} lines.

C. The external mode region

In this frequency region, nine modes at most could be detected: the three PF_6 librations, the three TMTSF parallel librations, and the three external relative motions of TMTSF. The PF_6 librations (one A_g and two B_g modes) are quite presumably invisible because the PF_6 anion has more or less a cubic symmetry. On the other hand, the TMTSF molecules are fairly anisotropic and the main Raman scattering mechanism for a libration is the rigid rotation of the molecular dielectric tensor.[15] Due to the approximate C_{2h} symmetry of the crystal, one expects two B_g libration modes in the VH spectrum (corresponding to rotations around axes perpendicular to a) and one A_g libration visible in the VV spectrum. Furthermore, the scattering mechanism for these modes involves the rigid rotation of the molecular orbitals and should have no resonant character. We can thus assume that the two modes at 36 and 64 cm^{-1} of the VH spectrum and the mode at 49 cm^{-1} of the VV spectrum (see Table II and Fig. 3), which are quite visible at 4545 Å, are three libration modes. Furthermore, we expect these modes to have the same intensity at all excitation wavelengths. We have taken them as intensity references and adjusted the unknown intensity ratio between the 4545- and 6471-Å spectra using this internal standard. This appears to give a coherent result for the two VH modes (see Fig. 3). Unfortunately, no check can be made on the VV spectrum (due to the relatively very intense 54-cm^{-1} mode at 6471 Å), but the result is certainly not grossly inconsistent. This intensity ratio has been used later on to draw Figs. 2, 3, and 4.

TABLE II. Frequencies (cm^{-1}) and assignments of the external modes.

Frequency (cm^{-1})	External mode
36	Libration B_g
46	Translation B_g
49	Libration A_g
52	Translation A_g
57	Translation B_g
64	Libration B_g

Let us now discuss the three translational modes. One A_{1g} mode is expected in the VV geometry and corresponds to a motion along a, while two B_g modes are expected in the VH spectrum, corresponding to motions perpendicular to this axis. Figure 3 shows that, among the three yet unidentified modes of this spectrum, only the 54-cm^{-1} mode is clearly resonating, in the VV geometry, at 6471 Å. This is exactly what we expected from Grant's calculation,[12] because the relative change of the LCMO transfer integral under pressure is just the electron-phonon matrix element (for $c_1=c_2$) of Eq. (1). As one transfer integral relative change is 4 times larger than any other and is related to a motion parallel to a, the corresponding mode should resonate 16 times more than the two other optical phonons. This mode can thus be safely identified with the internal relative displacement of the molecules along a. The only troublesome aspect is related to the VH spectrum, in which, under resonant conditions, the 54-cm^{-1} mode also appears, though less strongly. The breakdown of the C_{2h} symmetry is, of course, not surprising because this is only an approximate result. Nevertheless, this VH detection does not go along with the discussion in Sec. IV A and suggests that a transfer integral between a conduction-band molecular orbital and another unoccupied molecular orbital of a nearest neighbor is also very sensitive to a relative motion of the two molecules along a. Though this is not unlikely, there is no calculation at the present time to confirm our hypothesis.

Finally, two weak modes at 46 and 57 cm^{-1} appear in the VH spectrum and have no resonant character. We have tentatively attributed them to the two other optical translation modes of TMTSF, and our attribution of the whole low-frequency spectrum is given in Table II.

D. The 1400–1620-cm^{-1} spectral region

The five frequencies detected in this spectral range are reported in Table I. Three belong to the a_{1g} symmetry and have already been discussed in Sec. IV B, as well as already having reported the existence of an unidentified line at 1582 cm^{-1}. One more unsolved problem remains in this frequency range. Firstly, if the intensity ratio of the VV to the VH spectrum at 6471 Å is very similar to that of the lower part of the spectrum, this is not true for the 4545 Å spectra—both are equally intense. Secondly, in the latter case, not only is the 1463-cm^{-1} line more intense in the VH spectrum, but this is even more striking for the 1565-cm^{-1} line and also the 1479-cm^{-1} line (see Fig. 2), which explains why these lines have been reported on column 5 of Table I. Even if the Jacobsen optical-reflectance measurement suggests that one is approaching a new electronic resonance below 4000 Å, it is not clear why this would affect most specifically that part of the spectrum and would be more important in the VH spectrum.

V. SUMMARY AND FINAL REMARKS

The Raman experiments reported in this paper indicate that the main difficulty related to this experimental technique is the optical opaqueness of the $(TMTSF)_2PF_6$ crystals. This prevents the detection of any internal mode related to the PF_6 counteranion and practically any internal mode of TMTSF when one is not in a resonant Raman scattering condition: the only clearly visible modes in a nonresonant condition are the 1463-cm^{-1} line, which is strongly connected to the charge transfer mechanism, and the three TMTSF libration modes, which had not been previously detected. Under RRS conditions, nearly all the internal a_{1g} modes become visible and their frequencies agree, in general, with the valence force field calculation of Meneghetti *et al.*[6] Furthermore, an *external* optic mode related to a motion of the TMTSF molecules along the *a* (stacking) direction strongly resonates. The relative motion of the two molecules which is related to this mode is by definition the motion deeply involved in the charge transfer mechanism. The detection and identification of this mode is of great importance in the future understanding of the charge transfer mechanism and, possibly, of the superconducting properties of the other salts of the same family.

If the general picture which emerges from the present analysis is rather consistent, some findings remain unexplained. There exist unidentified resonant Raman scattering modes, and some of them are among the most intense of the RRS spectrum. Furthermore, in the 1450–1650-cm^{-1} region, a new resonance mechanism seems to take place when the laser frequency increases. Further experiments are clearly needed to elucidate these points.

ACKNOWLEDGMENTS

We would like to thank Dr. D. Jerome and his collaborators for providing us with the necessary crystals and for giving us the necessary advice for their manipulation. In particular, the constant help of Dr. C. Weyl in the preparation of the experiment and in guidance through the vast literature on these materials has been invaluable. The Département de Recherches Physiques at the Université Pierre et Marie Curie is a "Unité Associée au Centre National de la Recherche Scientifique, No. 71."

[1]D. Jerome, A Mazaud, M. Ribault, and K. Bechgaard, J. Phys. (Paris) Lett. **41**, L95 (1980).

[2]N. Thorup, G. Rindorf, H. Soling, and K. Bechgaard, Acta Crystallogr. Sect. B **37**, 1236 (1981).

[3]M. Ribault, J. P. Pouget, D. Jerome, and K. Bechgaard, J. Phys. (Paris) Lett. **41**, L607 (1980).

[4]K. Bechgaard, K. Carneiro, F. B. Rasmussen, M. Olsen, G. Rindorf, C. S. Jacobsen, H. J. Pedersen, and J. C. Scott, J. Am. Chem. Soc. **103**, 2440 (1981).

[5]K. Iwahana, H. Kuzmany, F. Wudl, and E. Aharon-Shalom, Mol. Cryst. Liq. Cryst. **79**, 39 (1982).

[6]M. Meneghetti, R. Bozio, I. Zanon, C. Pecile, C. Ricotta, and M. Zanetti, J. Chem. Phys. **80**, 6210 (1984).

[7]P. V. Huong, C. Carrigou-Lagrange, J. M. Fabre, and G. Giral, *Raman Spectroscopy,* edited by J. Lascombe *et al.* (Wiley, New York, 1982), p. 447.

[8]R. Bozio, C. Pecile, K. Bechgaard, F. Wudl, and D. Nalewajek, Solid State Commun. **41**, 905 (1984).

[9]M. J. Rice, N. O. Lipari, and S. Stässler, Phys. Rev. Lett. **39**, 1359 (1977).

[10]C. S. Jacobsen, D. B. Tanner, and K. Bechgaard, Phys. Rev. B **28**, 7019 (1983).

[11]M. H. Whangbo, W. M. Walsh, Jr., R. C. Haddon, and F. Wudl, Solid State Commun. **43**, 637 (1982).

[12]P. M. Grant, Phys. Rev. B **26**, 6888 (1982).

[13]R. Loudon, Proc. R. Soc. London, Ser. A **275**, 218 (1963).

[14]A. K. Ganguly and J. L. Birman, Phys. Rev. **162**, 806 (1967).

[15]D. Fontaine and R. M. Pick, J. Phys. (Paris) **40**, 1105 (1979).